p38 Mitogen-Activated Protein Kinase-Dependent Transactivation of ErbB Receptor Family

A Novel Common Mechanism for Stress-Induced IRS-1 Serine Phosphorylation and Insulin Resistance

Rina Hemi,[1] Yafit Yochananov,[1,2] Ehud Barhod,[1,2] Michal Kasher-Meron,[1,3] Avraham Karasik,[1,3] Amir Tirosh,[1] and Hannah Kanety[1,3]

OBJECTIVE—Stress stimuli such as tumor necrosis factor (TNF) have been shown to induce insulin receptor substrate (IRS)-1 serine phosphorylation and insulin resistance by transactivation of ErbB receptors. We aimed at elucidating the potential role of p38 mitogen-activated protein kinase (p38MAPK) in mediating stress-induced ErbB receptors activation.

RESEARCH DESIGN AND METHODS—p38MAPK effect on ErbBs transactivation and insulin signaling was assessed in Fao or HepG2 cells, exposed to stress stimuli, and on metabolic parameters in *ob/ob* and C57/BL6 mice.

RESULTS—High-fat diet–fed mice and *ob/ob* mice exhibited elevated hepatic p38MAPK activation associated with glucose intolerance and hyperinsulinemia. Liver expression of dominant-negative (DN)-p38MAPKα in *ob/ob* mice reduced fasting insulin levels and improved glucose tolerance, whereas C57/BL6 mice overexpressing wild-type p38MAPKα exhibited enhanced IRS-1 serine phosphorylation and reduced insulin-stimulated IRS-1 tyrosine phosphorylation. Fao or HepG2 cells exposed to TNF, anisomycin, or sphingomyelinase demonstrated rapid transactivation of ErbB receptors leading to PI3-kinase/Akt activation and IRS-1 serine phosphorylation. p38MAPK inhibition either by SB203580, by small interfering RNA, or by DN-p38MAPKα decreased ErbB receptors transactivation and IRS-1 serine phosphorylation and partially restored insulin-stimulated IRS-1 tyrosine phosphorylation. When cells were incubated with specific ErbB receptors antagonists or in cells lacking ErbB receptors, anisomycin- and TNF-induced IRS-1 serine phosphorylation was attenuated, despite intact p38MAPK activation. The stress-induced p38MAPK activation leading to ErbB receptors transactivation was associated with intracellular reactive oxygen species generation and was attenuated by treatment with antioxidants.

CONCLUSIONS—Hepatic p38MAPK is activated following various stress stimuli. This event is upstream to ErbB receptors transactivation and plays an important role in stress-induced IRS-1 serine phosphorylation and insulin resistance. ***Diabetes*** **60:1134–1145, 2011**

From the [1]Institute of Endocrinology, Chaim Sheba Medical Center, Tel-Hashomer, Israel; the [2]Mina and Everard Goodman Faculty of Life Sciences, Bar-Ilan University, Ramat-Gan, Israel; and the [3]Sackler Faculty of Medicine, Tel Aviv University, Tel Aviv, Israel.

Corresponding author: Hannah Kanety, hkanety@sheba.health.gov.il.

Received 4 September 2009 and accepted 20 January 2011.

DOI: 10.2337/db09-1323

This article contains Supplementary Data online at http://diabetes.diabetesjournals.org/lookup/suppl/doi:10.2337/db09-1323/-/DC1.

R.H., Y.Y., and E.B. contributed equally to this work.

Insulin resistance has been strongly associated with obesity (1) and a variety of pathological stress conditions, including inflammatory diseases, hemorrhage, thermal injury, sepsis, and cancer cachexia (2–5). These pathological states are characterized by increased inflammatory response as indicated by high levels of proinflammatory cytokines, such as tumor necrosis factor (TNF)-α (6–8). Numerous studies have demonstrated the central role of TNF in obesity-induced insulin resistance by promoting Ser phosphorylation of insulin receptor (IR) substrate (IRS)-1, which impairs IR-IRS-1 interaction compromising insulin signal propagation (9–11). These cellular effects of TNF had been suggested to be mediated by the sphingomyelin pathway as evident by the effects of sphingomyelinase (SMase) and cell-permeable ceramide analogs (11,12).

Increased IRS-1 Ser phosphorylation and impaired metabolic responses to acute insulin stimulation in cellular systems representing liver, skeletal muscle, and adipose tissues were demonstrated not only in response to TNF but also as a consequence of additional stress stimuli, such as oxidative conditions (13,14), osmotic shock, and the translation inhibitor anisomycin (AN) (15–17). However, the downstream pathways linking between the various stress-stimuli and increased IRS-1 Ser phosphorylation are not fully elucidated. The activation of p38 mitogen-activated protein kinase (p38MAPK) has been suggested as one potential candidate for mediating IRS-1 Ser phosphorylation by cellular stresses, although not directly, mainly by in vitro studies demonstrating improvement of stress-induced insulin resistance with pharmacological p38MAPK inhibitors (18–20).

Previously, we have demonstrated that stress stimuli such as TNF and AN promote ligand-independent transactivation of ErbB2 and ErbB3 receptors (members of the epidermal growth factor [EGF]/ErbB family of receptor Tyr-kinases), resulting in their association with the p85-subunit of PI3-kinase (PI3K) and augmented PI3K activity. Stimulation of the PI3K signal cascade, downstream to ErbB receptors, induced Ser phosphorylation of IRS proteins and promoted insulin resistance (16). Since p38MAPK activation, a central component of the stress response (21), was demonstrated to be linked to the ErbB family activity in several cellular models (22,23), we aimed at assessing the potential role of p38MAPK activation in ErbB receptors mediated hepatic insulin resistance.

In the current study we provide evidence in various models that stress-induced activation of p38MAPKα in the

liver is an upstream event, crucial for transactivation of the ErbB receptors leading to IRS-1 Ser phosphorylation and desensitization of insulin signaling.

RESEARCH DESIGN AND METHODS

Cell culture studies. Rat hepatoma Fao and human hepatoma HepG2 cells were grown in RPMI-1640 and Dulbecco's modified Eagle's medium (DMEM), respectively, supplemented with 10% FCS. Confluent monolayers, deprived of serum for 16 h, were incubated without or with SMase (neutral, *Staphylococcus aureus*), TNF, or AN at the indicated concentrations and time intervals and then stimulated for the indicated times without or with 100 nmol/L insulin. In glucose oxidase (GO; Sigma) experiments, GO was added to serum-free RPMI-1640 medium for 10 min at 37°C to generate H_2O_2 and then added to cells at the indicated concentrations and time intervals. In some experiments, cells were treated without or with different signaling inhibitors (LY294002, PD168393, SB203580, PD98059, AG825 [Calbiochem]) for 30 min or with various antioxidants (*N*-acetyl-L-cysteine [NAC], glutathione [GSH], diphenyleneiodoniumchloride [DPI] [Sigma]) for 1 h at the indicated concentrations before incubation without or with stress stimuli and insulin. Cells were solubilized at 4°C with buffer A (Supplementary Data). After three freeze-thaw cycles, cell extracts were centrifuged (12,000*g*, 30 min, 4°C) and supernatants were collected as the cytosolic fraction. Resulting pellets were solubilized with buffer B (Supplementary Data) and supernatants (12,000*g*, 15 min, 4°C) were collected as the particulate fraction. Total cell extracts were prepared by solubilizing cells with buffer B. Following separation by SDS-PAGE, proteins were subjected to Western immunoblotting with antibodies directed against IR, IRS-1 (16), ErbB2-phospho-(p)Tyr^{1248}, IRS-1-pSer^{307}, p85-PI3K (Upstate Biotechnology), pTyr (Transduction Laboratories), ErbB3-pTyr^{1289}, Akt-pSer^{473}, IRS-1-pSer^{612}, IRS-1-pSer$^{636/639}$, MAPKAPK2-pThr^{334} (Cell Signaling Technology), p38MAPK-Thr^{180}/Tyr^{182}, α-tubulin, MKK-3/6-pSer$^{189/207}$, MKK-3 (Sigma), ErbB1, ErbB2, ErbB3, p38MAPK (Santa Cruz Biotechnology), ErbB1-pTyr^{1086}, ErbB1-pTyr^{1173}, and IRS-1-pTyr^{612} (Biosource). Ser^{307}, Ser^{612}, Ser^{632}, and Tyr^{608} in rat IRS-1 are equivalent to Ser^{312}, Ser^{616}, Ser^{636}, and Tyr^{612} in human IRS-1, respectively.

Adenoviruses. The DN-p38MAPKα (Ad.p38/AF, the AF mutant cannot be phosphorylated, since the TGY dual phosphorylation site has been changed to AGF) and wild-type (WT)-p38MAPKα adenoviruses, constructed as described (24), were provided by Dr. Jiahuai Han. β-Galactosidase (β-gal) adenovirus, used as control in all experiments, was obtained from Cell Biolabs. Viral titters were determined by QuickTiter adenovirus titer immunoassay kit (Cell Biolabs).

Cells infection with adenoviral constructs. Cells were infected with adenoviruses at multiplicity of infection (MOI) as indicated, and experiments were performed 48 h after infection. Infection efficiency was 70–80% as determined by green fluorescent protein (GFP)-adenovirus.

Gene silencing. Fao or HepG2 cells were transfected by 100 nmol/L rat p38MAPKα or human ErbB1 *SMART*pool small interfering RNAs (siRNAs) (Dharmacon). Nontargeted siRNA was used as control. Experiments were performed 96 h after transfection.

Growing Fao cells at various cell densities. Confluent Fao cells, grown in 90-mm plates, were divided into three (cell density-1) or forty-eight (cell density-1/16) 60-cm plates. After 48 h, cells were treated with 50 ng/mL AN for 30 min and assayed as indicated above.

Immunoprecipitation. Cell extracts were incubated (2–12 h, 4°C) with the indicated antibodies. ErbB2/ErbB3 heterodimer immunoprecipitation was performed by using a mixture of anti-ErbB2 (2 μg) and anti-ErbB3 antibodies (2 μg). Immunocomplexes were incubated (1 h, 4°C) with protein G/A-Sepharose beads mixture, collected, washed three times with buffer B, and subjected to SDS-PAGE following immunoblotting with the indicated antibodies.

IRS-1 binding to immobilized IR. IR was purified from Fao cells on a wheat-germ agglutinin (WGA) coupled to agarose (16). Immobilized IR was incubated (2 h, 4°C) with cytosolic extracts derived from Fao cells treated with AN or SMase. IR-IRS-1 binding was determined as previously described (16).

PI3K assay. Total extracts were immunoprecipitated using p85-PI3K or mixture of ErbB2/ErbB3 antibodies. PI3K activity in the immunocomplexes was determined as previously described (16).

Reactive oxygen species production. Cells, washed twice in RPMI-1640 medium without phenol red, were incubated at 37°C in medium containing 5 μM of reactive oxygen species (ROS) sensitive fluorescent dye, dichlorofluorescein (CM-DCF). After 1 h, cells were washed with PBS and fluorescence was immediately measured in a plate reader (Tecan) with an excitation/emission wavelength of 485/515 nm.

Animal studies. C57/BL6 male mice 8 or 10 weeks old and 8-week-old *ob/ob* male mice (Harlan Laboratories) were maintained on a 12-h light/dark cycle. All protocols for animal uses were reviewed and approved by the Animal Care Committee of the Sheba Medical Center and were in accordance with Institutional Animal Care and Use Committee guidelines.

DN-p38MAPKα, WT-p38MAPKα, and β-gal (control for viral infection) adenoviruses were injected into mice through the tail vein (200 μL of 1–30 × 10^{10} ifu/mL, diluted in PBS). Noteworthy, systemic glucose homeostasis and hepatic IR, IRS-1, and Akt protein levels were not significantly different in β-gal-infected mice compared with noninfected mice (Supplementary Fig. 1), unlike recent findings in rats (25). Quantitative real-time PCR (qPCR) analysis (Supplementary Data) exhibited a specific expression of p38MAPK, delivered by the adenoviruses, in the liver but not in skeletal muscle. Intraperitoneal glucose tolerance tests (IPGTT) were performed 5 days after adenovirus injection by using 2 g glucose/kg of body weight after a 6- or 12-h fast. Blood glucose values were determined with a glucose-meter (Bayer). Plasma aliquots were obtained 1 day post GTT and after 6- or 12-h fasting, as indicated, and stored at −20°C. Insulin levels were determined by ultra-sensitive mouse insulin ELISA kit (Mercodia).

Insulin signaling in vivo. Insulin signaling in vivo was performed by injecting 2 mU insulin/g body weight in the portal vein of anesthetized animals. Animals were killed 5 min later, and the liver was harvested, frozen in liquid nitrogen, and stored at −80°C before further analysis.

Tissue extraction. Liver tissues from adenoviral-infected mice harvested 6 days after adenovirus injection and from high-fat diet–fed mice (HFD; 42% kcal from fat for 20 weeks or 60% kcal from fat for 8 weeks) were homogenized in Buffer B. Protein extracts were used for immunoblotting as described above.

Statistical analysis. All data are expressed as mean ± SE. Two-tailed Student *t* tests were performed on data at a minimum $P < 0.05$ threshold.

RESULTS

p38MAPKα mediates insulin resistance in vivo. In agreement with previous observations (26,27), both *ob/ob* mice as well as C57/BL6 mice fed with HFD demonstrated elevated liver p38MAPK activity (two- to threefold), compared with lean C57/BL6 mice, as indicated by its increased phosphorylation (Fig. 1*A*). To assess the role of p38MAPK in mediating hepatic insulin resistance in these models, we over-expressed DN-p38MAPKα or β-gal, a control adenovirus, in the liver of *ob/ob* mice by tail vein injection of adenoviral-based expression vectors (Fig. 1*B–E* and Supplementary Fig. 2, representing two independent experiments). Overexpression of DN-p38MAPKα resulted in a significant decrease in hepatic p38MAPK activation (1.7-fold, Fig. 1*B*, and 1.9-fold, Supplementary Fig. 2*A*), measured at day 6 post adenovirus administration. The difference in p38MAPK activity among the DN-p38MAPKα and the β-gal injected mice closely resembled differences observed in p38MAPK activation between obese and lean mice.

GTT, performed 5 days after adenovirus administration, revealed a significant improvement in glucose tolerance in mice overexpressing DN-p38MAPKα (Fig. 1*C*, Supplementary Fig. 2*C*). In addition, fasting insulin levels were considerably lower in the DN-p38MAPKα expressing mice compared with β-gal controls (Fig. 1*D*), indicating improved insulin sensitivity. qPCR analysis revealed that DN-p38MAPKα overexpression in the liver resulted in a significant downregulation of phosphoenolpyruvate carboxykinase (PEPCK), one of the key enzymes involved in gluconeogenesis (Fig. 1*E*, Supplementary Fig. 2*D*).

To further support the importance of liver p38MAPK in mediating insulin resistance, lean C57/BL6 mice were injected via the tail vein with adenoviruses that express WT-p38MAPKα or β-gal. As demonstrated in Fig. 2*A*, mice overexpressing WT-p38MAPKα exhibited increased p38MAPK activation in the liver, accompanied by increased phosphorylation of IRS-1 on Ser^{612} and Ser^{632} residues (Fig. 2*B*). Signaling studies performed after acute injection of either saline or insulin for 5 min revealed that WT-p38MAPKα overexpression in liver reduced insulin ability to stimulate both Tyr phosphorylation of IRS-1 (Tyr^{608}) and Akt activation (Fig. 2*C*). As shown in Fig. 2*D*, there was no significant difference in glucose tolerance

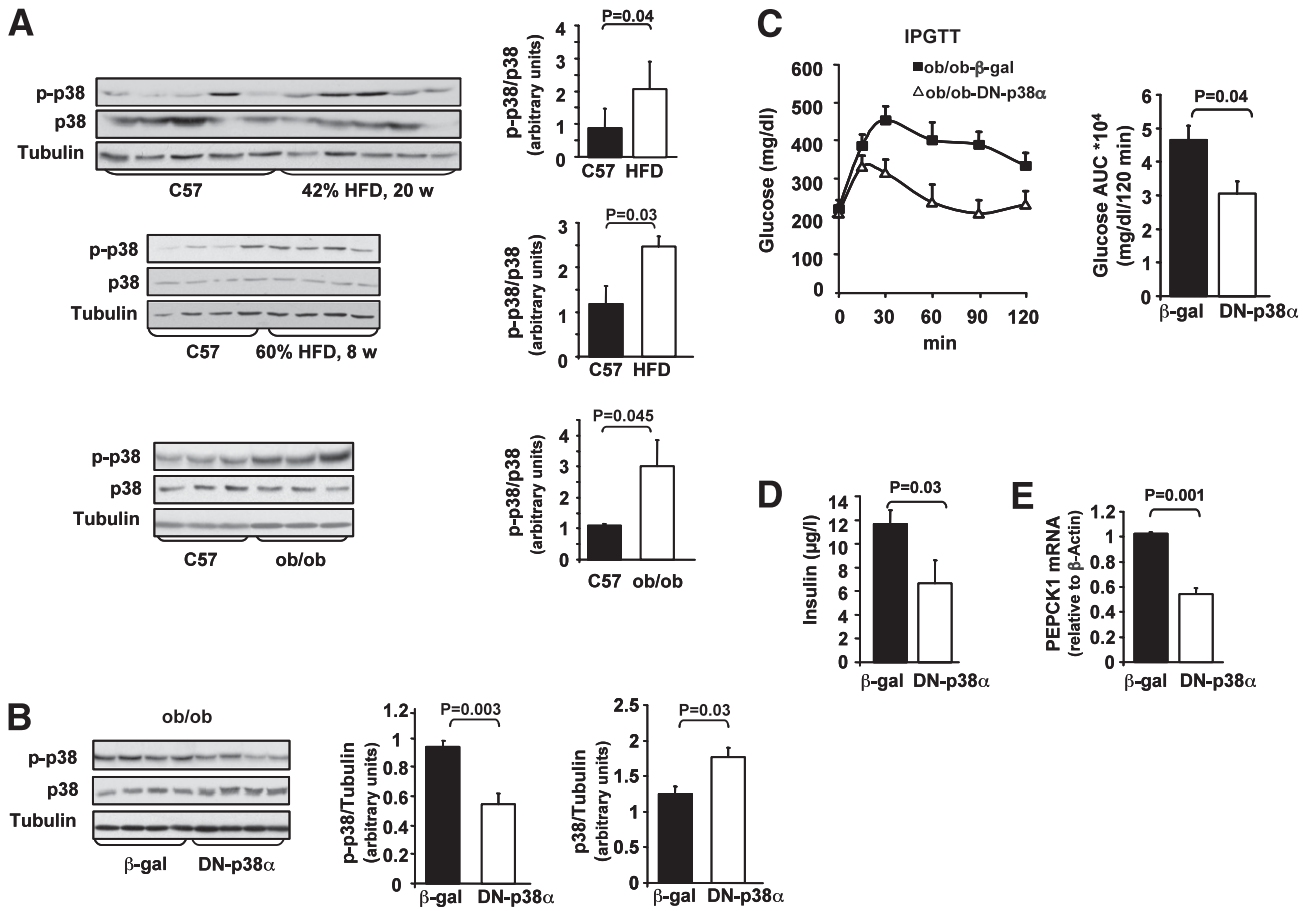

FIG. 1. Effects of adenoviral DN-p38MAPKα overexpression in the liver, on insulin resistance, and glucose intolerance in obese mice models. *A*: The levels of hepatic p38MAPKα (p38), *p*-p38MAPK (*p*-p38), and α-tubulin were assessed in C57/BL6 (C57) mice fed with standard diet or HFD and in *ob/ob* mice, using Western blot analysis. Quantification of *p*-p38 and p38 immunoblots was performed using ImageJ analysis. Results are expressed as *p*-p38 relative to p38 in control (n = 5) and HFD (n = 5) mice or in control (n = 3) and *ob/ob* (n = 3) mice and are presented as the means ± SE. *B: ob/ob* mice were injected with β-gal (n = 6) or DN-p38α (n = 6) adenoviral constructs via tail vein. Levels of p38α, *p*-p38, or α-tubulin in the liver were assessed using Western blot analysis. Quantification of immunoblots was performed using ImageJ analysis. The results are expressed as *p*-p38 or p38 relative to the loading control (α-tubulin) and are presented as the means ± SE. *C*: IPGTT was performed 5 days after adenovirus injection, after a 6-h fast. The area under the curve (AUC) was estimated by summing the numerical integration values of successive linear segments of the glucose curve for 0–15, 15–30, 30–60, 60–90 and 90–120 min. *D*: Blood insulin levels were measured after 6-h fasting. *E*: PEPCK1 mRNA expression was assessed by qPCR.

between WT-p38MAPKα-treated and β-gal-treated mice. Nevertheless, fasting insulin levels were significantly higher in WT-p38MAPKα expressing mice compared with β-gal controls (Fig. 2*E*), indicating that p38MAPKα overexpression increases insulin resistance. Expression levels of PEPCK were increased (45%) by WT-p38MAPKα treatment compared with β-gal controls, although this difference did not reach statistical significance (P = 0.25). Similar findings were reported in mice overexpressing WT-Jun NH_2-terminal kinase (JNK) in the liver (28).

p38MAPK mediates stress-induced IRS-1 Ser phosphorylation leading to insulin signal desensitization. To further test the potential role of p38MAPK in the development of hepatic insulin resistance, we evaluated the effect of promoting or suppressing p38MAPK activity on IRS-1 Ser phosphorylation and insulin signal transduction in vitro. For these studies we used human HepG2 (Fig. 3*A–C*) and rat Fao (Fig. 3*D–G*) hepatoma cells treated with known inducers of insulin resistance such as TNF, SMase, or AN (11,16). The efficacy of the various methodologies used to manipulate p38MAPK activity was confirmed by evaluating the phosphorylation of p38MAPK or its downstream substrate MAPKAPK2.

Incubation of HepG2 cells with TNF increased p38MAPK activation and IRS-1 Ser phosphorylation as demonstrated for $Ser^{636/9}$ and Ser^{312} (Fig. 3*A*), accompanied by decreased ability of insulin to promote IRS-1 Tyr phosphorylation (Fig. 3*B*). Overexpression of WT-p38MAPKα enhanced TNF effect on IRS-1 Ser phosphorylation (Fig. 3*A*), leading to further deterioration in insulin signaling (Fig. 3*B*), whereas inhibiting p38MAPKα activation by DN-p38MAPKα adenovirus infection (Fig. 3*A* and *B*) or pharmacologically by SB203580 (Fig. 3*C*) attenuated TNF effects.

Similar to our observations in HepG2, incubation of Fao cells with AN or SMase increased IRS-1 phosphorylation on Ser^{632}, Ser^{612}, and Ser^{307} (Fig. 3*D–F*). Inhibition of stress-induced p38MAPK activation, either by DN-p38MAPKα overexpression (Fig. 3*D*), by knockdown of p38MAPKα expression with specific siRNA sequences (Fig. 3*E*), or by SB203580 (Fig. 3*F*) resulted in significant reduction in IRS-1 phosphorylation on these residues. As expected, IRS-1 Ser phosphorylation, induced by either AN or SMase, led to decreased ability of insulin to promote IRS-1 Tyr phosphorylation (Fig. 3*G*, *upper panels*), because of impaired interaction of Ser phosphorylated IRS-1 with the IR (Fig. 3*G*, *lower panel*), as assessed by in vitro interaction assay (16).

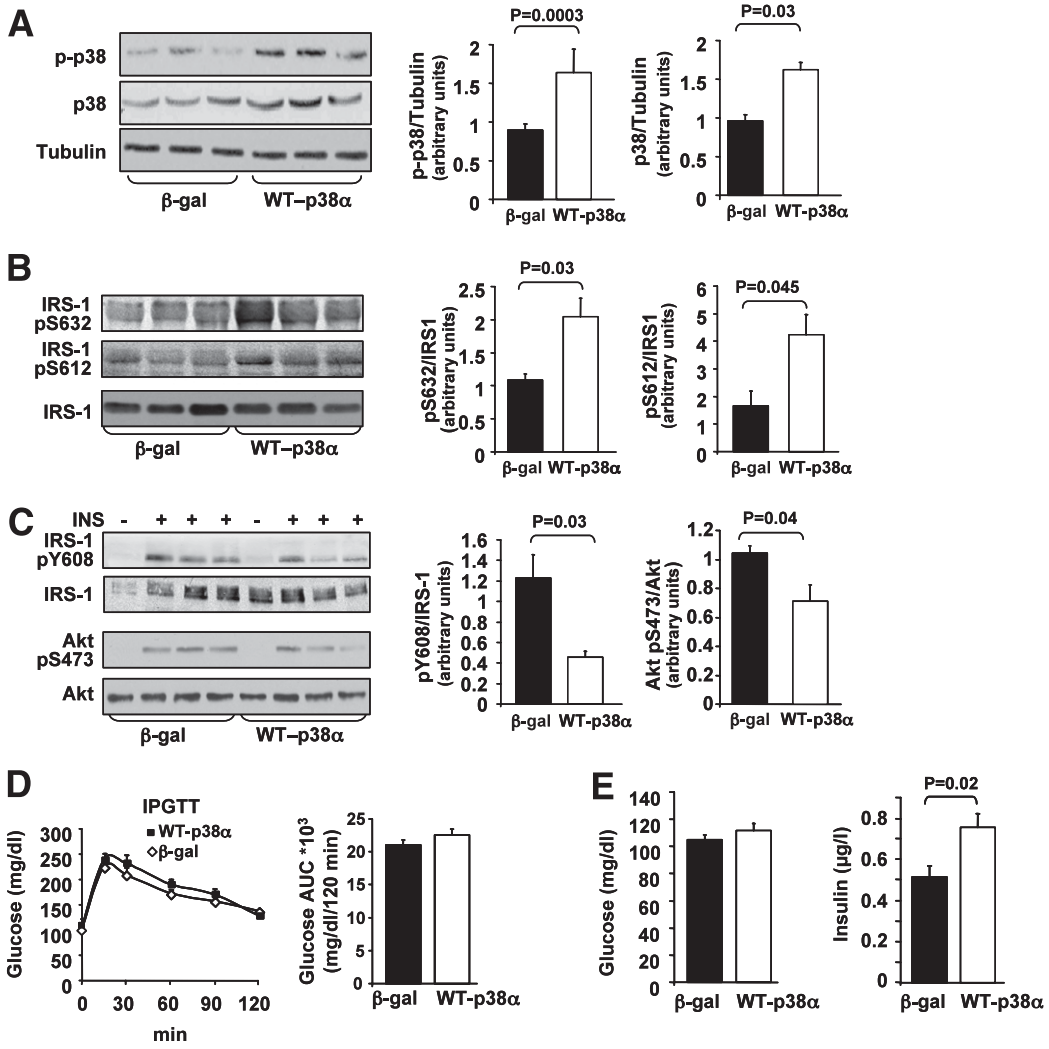

FIG. 2. Effects of adenoviral p38MAPKα overexpression in the liver, on insulin signaling, and glucose tolerance in C57/BL6 mice. *A*: C57 male mice were infected with β-gal (n = 15) or WT-p38α (n = 15) adenoviral constructs via tail vein injection. The levels of p38α, *p*-p38, and α-tubulin in the liver were assessed using Western blot analysis. Quantification of immunoblots was performed using ImageJ analysis. The results are expressed as *p*-p38 or p38 relative to the loading control (α-tubulin) and are presented as the means ± SE. *B*: Levels of IRS-1-pSer^{632}, IRS-1-pSer^{612}, and IRS-1 in the liver were determined by immunoblotting with specific antibodies as indicated. Quantification of immunoblots was performed using ImageJ analysis. The results are expressed as IRS-1-pSer^{632}, IRS-1-pSer^{612}, relative to IRS-1, and are presented as the means ± SE. *C*: Mice infected with β-gal (n = 5) or with WT-p38α (n = 5) adenoviral constructs were treated with insulin as described in RESEARCH DESIGN AND METHODS. Insulin-induced Tyr phosphorylation of IRS-1 and Akt activation was analyzed by antibodies against IRS-1-pTyr^{608}, IRS-1, Akt-pSer^{473}, and Akt. Quantification of immunoblots was performed using ImageJ analysis. The results are expressed as IRS-1-pTyr^{608} relative to IRS-1 and Akt-pSer^{473} relative to Akt and are presented as the means ± SE. *D*: IPGTT was performed 5 days after adenovirus injection, after 12-h fasting. The AUC was estimated as described in Fig. 1*C*. *E*: Blood glucose and insulin levels were measured after 12-h fasting.

Inhibition of stress-induced p38MAPK activation restored both IR-IRS-1 interaction and the subsequent Tyr phosphorylation of IRS-1 (Fig. 3*G*).

p38MAPK activation mediates stress-induced ErbB receptors transactivation. Previously we have demonstrated the importance of ErbB receptors transactivation in stress-induced insulin resistance. Our findings revealed that activation of a PI3K cascade, downstream to ErbB receptors by cellular stressors, induces Ser phosphorylation of IRS proteins culminating in insulin signaling desensitization (16).

To assess the role of p38MAPK in mediating insulin resistance in an ErbB-dependent manner, we evaluated the effect of inhibiting or augmenting p38MAPK activity on ErbB receptors activation in both Fao (Fig. 4) and HepG2 (Fig. 5*A*–*C*) cells. In accordance with our previous findings, Tyr phosphorylation of ErbB2 and ErbB3, the predominant ErbB receptors in Fao cells (16), could be detected following 5- to 10-min incubation with AN or SMase (Fig. 4*A*, *upper panels*). Stress-induced p38MAPK activation followed a similar time course (Fig. 4*A*, *lower panels*). As depicted in Fig. 4*B*, silencing of p38MAPKα suppressed AN-induced ErbB2/ErbB3 Tyr phosphorylation, as demonstrated for ErbB2-Tyr^{1248}, one of the major ErbB2 autophosphorylation sites, and ErbB3-Tyr^{1289}, one of the six ErbB3 binding sites for the p85-subunit of PI3K. Similarly, inhibition of p38MAPK activation, induced by the various stress stimuli, using either DN-p38MAPKα overexpression (Fig. 4*C*) or SB203580 (Fig. 4*D* and Supplementary Fig. 3*A*), effectively reduced ErbB2/ErbB3 total Tyr phosphorylation, as well as ErbB2 phosphorylation on Tyr^{1248}. Moreover, parallel to the efficient reduction in AN-induced ErbB2/ErbB3 Tyr phosphorylation by SB203580, a significant reduction in ErbB2/ErbB3-associated PI3K

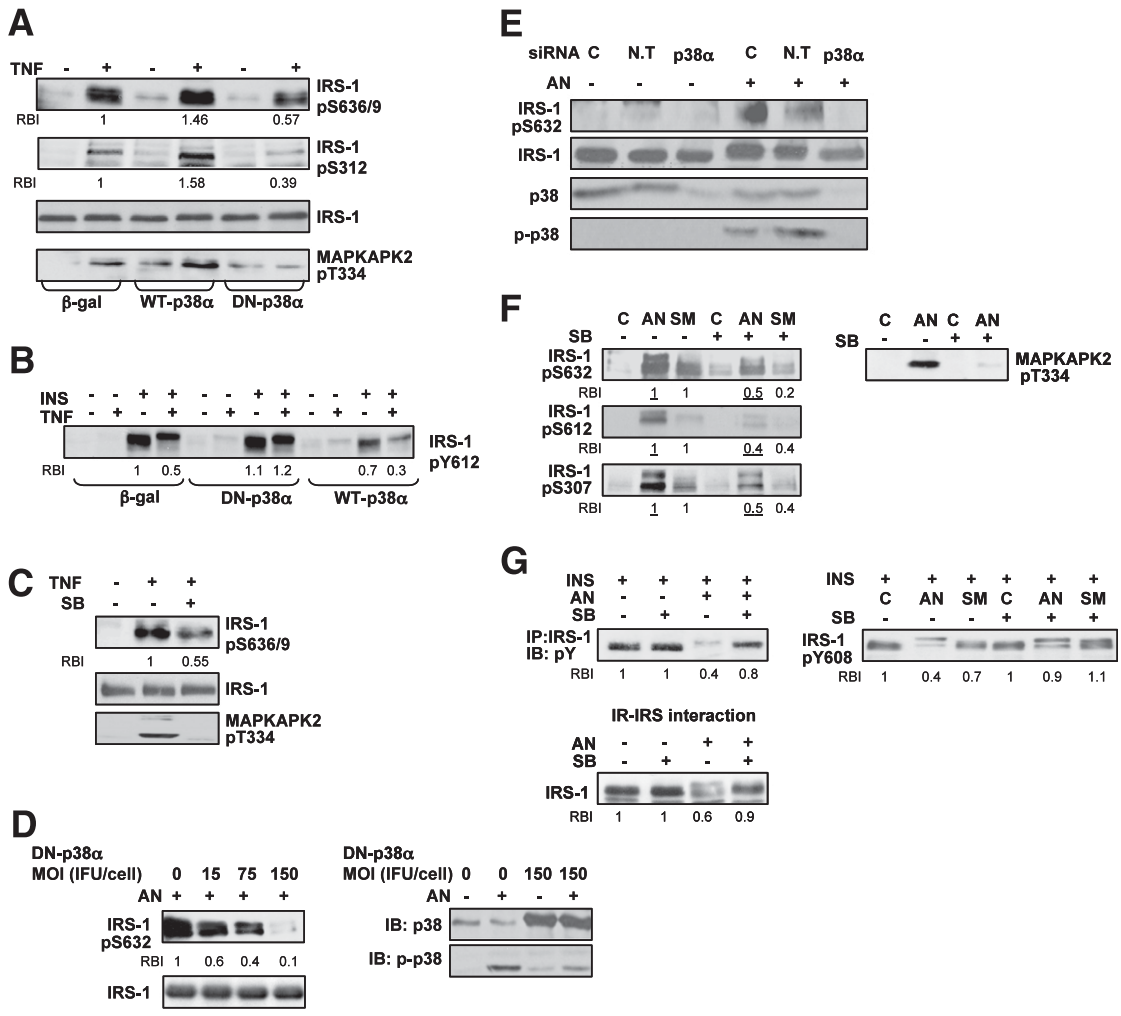

FIG. 3. p38MAPK mediates stress-induced IRS-1 Ser phosphorylation leading to insulin signal desensitization. HepG2 cell experiments: *A*: Cells infected with 15 MOI (ifu/cell) of β-gal, DN-p38α, and WT-p38α adenoviral constructs for 48 h were treated without or with 5 nmol/L TNF for 30 min. Total cell extract proteins were resolved by SDS-PAGE and then immunoblotted with antibodies as indicated. *B*: Cells infected as in *A* were treated without or with 5 nmol/L TNF for 30 min and then incubated without or with 100 nmol/L insulin for 5 min. Total cell extracts proteins were analyzed by immunoblot analysis using anti-IRS-1-pTyr^{612} antibodies. *C*: Cells were treated without or with 10 μmol/L SB203580 (SB) for 30 min, before incubation with 5 nmol/L TNF for 30 min. Total cell extract proteins were analyzed by immunoblot analysis using anti-IRS-1-pSer$^{636/9}$, anti-IRS-1, and anti-MAPKAPK2-pThr^{334} antibodies. Fao cell experiments: *D* and *E*: Cells infected DN-p38α adenoviral constructs at the indicated MOI (ifu/cell) for 48 h (*D*), or transfected by p38α or nontargeted (N.T) siRNA for 96 h (*E*), were treated without or with 50 ng/mL AN for 30 min. IRS-1-pSer^{632}, IRS-1, *p*-p38, and p38 in total cell extract proteins were examined with immunoblot analysis using the indicated antibodies. *F*: Cells were treated without or with 10 μmol/L SB203580 for 30 min, before incubation without or with 300 mU/mL SMase or 50 ng/mL AN for 30 min at 37°C. Total cell extract proteins were resolved by SDS-PAGE, and then immunoblotted with antibodies as indicated. *G*: Protein extracts from Fao cells treated as described above were incubated without or with 100 nmol/L insulin for 1 min. Proteins from cell lysates were immunoprecipitated with anti-IRS-1 antibodies, resolved by SDS-PAGE, and immunoblotted with anti-pTyr antibodies (*G*, *upper left panel*) or directly resolved by SDS-PAGE and then immunoblotted with IRS-1-pTyr^{608} antibodies (*G*, *upper right panel*). Cytosolic proteins from cells treated without or with SB203580 before incubation without or with AN as described above were bound to immobilized IR. IR-IRS complexes were subjected to immunoblot analysis with anti IRS-1 antibodies (*G*, *lower panel*). Each panel in *A*–*G* represents three to five independent experiments. In each panel, the relative band intensity (RBI) of a given band presents the means of three to five independent experiments. Band intensity measurements were performed using ImageJ analysis.

activity and Akt-Ser^{473} phosphorylation was observed (Fig. 4*E*).

We next evaluated the involvement of p38MAPK in stress-induced ErbB receptors transactivation in HepG2 cells. TNF promoted Tyr phosphorylation of ErbB1, the predominant ErbB receptor in these cells, as demonstrated by its increased phosphorylation on Tyr^{1173} and Tyr^{1086} residues (Fig. 5*A*), as well as Tyr phosphorylation of ErbB3, as demonstrated for Tyr^{1289} (Fig. 5*B*). This enhanced phosphorylation was accompanied by ErbB1 and ErbB3 association with the p85-subunit of PI3K (data not shown).

The transactivation of ErbB1 and ErbB3 by TNF was significantly augmented with overexpression of WT-p38MAPKα but attenuated in cells overexpressing DN-p38MAPKα (Fig. 5*A*) or by SB203580 (Fig. 5*B*). Moreover, p38MAPK inhibition by SB203580 resulted in a significant reduction in TNF-induced Akt-Ser^{473} phosphorylation (Fig. 5*C*). Noteworthy, whereas stress-induced ErbB receptors Tyr phosphorylation was attenuated by p38MAPK inhibition, their phosphorylation, stimulated by NDF-β1, an ErbB3 ligand, or by EGF, an ErbB1 ligand, was unaffected by SB203580 (Supplementary Fig. 3*B*). These results confirm that p38MAPK serves as an upstream mediator of stress-induced ErbB receptors transactivation.

When assessed in vivo, C57/BL6 mice, in which ErbB1 is the predominant ErbB in liver, exhibited significant

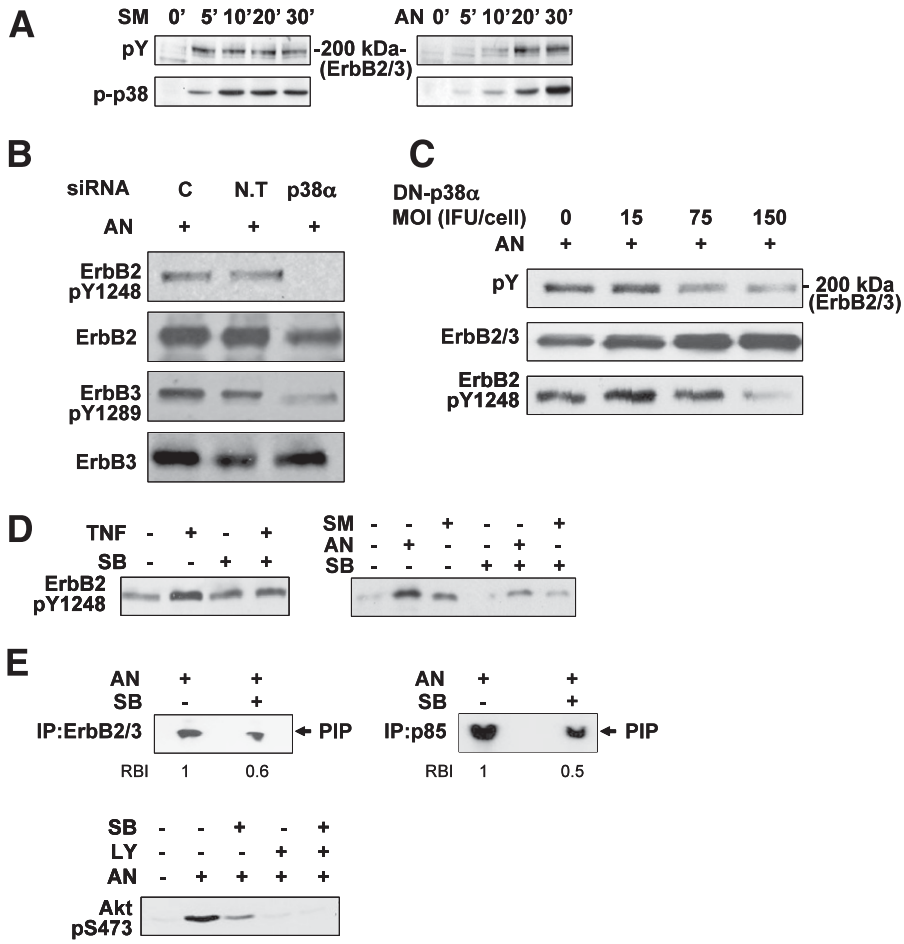

FIG. 4. p38MAPK involvement in stress-induced ErbB2/ErbB3 transactivation in Fao cells. *A*: Cells were incubated with 300 mU/mL SMase or 50 ng/mL AN for the indicated times at 37°C. Total cell proteins were analyzed by SDS-PAGE, and the blots were probed with anti-pTyr or anti-*p*-p38 antibodies. *B* and *C*: Cells transfected by p38α or nontargeted (N.T) siRNA for 96 h (*B*) or infected with DN-p38α adenoviral constructs at the indicated MOI (ifu/cell) for 48 h (*C*) were treated with 50 ng/mL AN for 30 min. ErbB2-pTyr^{1248}, ErbB3-pTyr^{1289}, pTyr, ErbB2, and ErbB3 in total cell extract proteins were examined with immunoblot analysis using the indicated antibodies. The levels of ErbB2 and ErbB3 (ErbB2/3) in *C*, *second panel*, were assessed by immunoblot analysis using a mixture of anti-ErbB2 and anti-ErbB3 antibodies (2 μg each). *D*: Cells were treated without or with 10 μmol/L SB203580 (SB) for 30 min, before incubation without or with 5 nmol/L TNF, 300 mU/mL SMase, or 50 ng/mL AN for 30 min at 37°C. Total cell extract proteins were analyzed by Western immunoblot analysis using anti-ErbB2-pTyr^{1248} antibodies. *E*: Cells were treated with 10 μmol/L SB203580 (SB) and 50 ng/mL AN as described above. Immunoprecipitation was performed using p85-PI3K or mixture of anti-ErbB2 and anti-ErbB3 antibodies and PI3K activity was measured as described in RESEARCH DESIGN AND METHODS (*E*, *upper panels*). Cells were treated without or with 25 μmol/L LY294002 (LY) or 10 μmol/L SB203580 (SB) for 30 min before incubation without or with 50 ng/mL AN for 30 min. Akt activation was analyzed by immunoblotting with anti-Akt-pSer^{473} antibodies (*E*, *lower panel*). Each panel in *A*–*E* contains a representative blot of at least three independent experiments. The RBI of a given band in *E*, *upper panels*, presents the means of three independent experiments. Band intensity measurements were performed using ImageJ analysis.

transactivation of ErbB1 following overexpression of WT-p38MAPKα, as indicated by a twofold increase in its Tyr^{1173} phosphorylation (Fig. 5*D*). Furthermore, hepatic expression of ErbB1 and ErbB3, as well as their Tyr phosphorylation on ErbB1-Tyr^{1173} and ErbB3-Tyr^{1289}, was significantly increased in C57/BL6 mice fed with HFD (Fig. 5*E*), in which elevated p38MAPK activity was demonstrated (Fig. 1*A*). Taken together, our findings support the notion that p38MAPK activation following stress stimuli is an essential upstream event in transactivation of distinct ErbB receptors, leading to impaired insulin action.

Incubation of Fao cells with insulin induces slow increase (20–60 min) in IRS-1 Ser phosphorylation leading to downmodulation of insulin receptor signaling (11). Because p38MAPK has been implicated in insulin signaling in H4IIE hepatoma cells (29,30), we next evaluated whether the p38MAPK-ErbB receptors pathway is activated by insulin itself, as part of its negative feedback control. Incubation of Fao cells with 100 nmol/L insulin for up to 60 min did not promote ErbB2/ErbB3 Tyr phosphorylation (Supplementary Fig. 4*A*). Additionally, in accordance with prior studies (26,31,32), insulin, unlike stress stimuli, had no significant effect on p38MAPK phosphorylation in Fao or HepG2 cells (Supplementary Fig. 4*B* and *C*). The discrepancy in p38MAPK activation by insulin, reported in the various liver cells (29–32), is unclear and may arise from different expression of MAPK phosphatases or other signals that attenuate p38MAPK activation by insulin (26).

Collectively, our findings support a role for p38MAPK-ErbB pathway in the negative feedback control mechanisms regulating hepatic insulin signaling under stress conditions but not under physiological conditions.

ErbB receptors are essential for p38MAPK-mediated IRS-1 Ser phosphorylation under stress conditions. To firmly confirm that ErbB receptors transactivation is a necessary event in p38MAPK-mediated insulin resistance

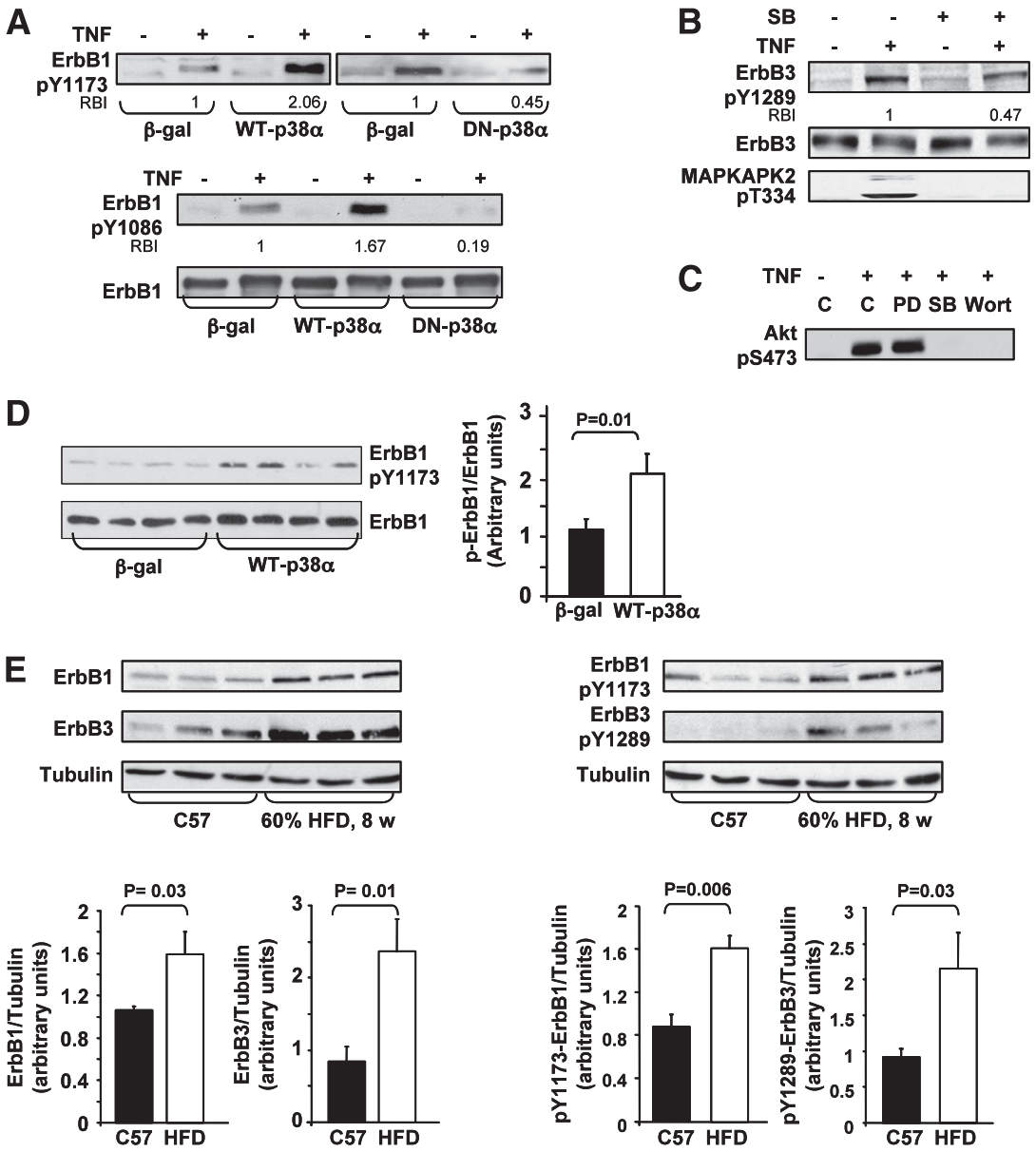

FIG. 5. p38MAPK involvement in stress-induced ErbB receptors transactivation in HepG2 cells and in C57/BL6 mice. HepG2 cell experiments: *A* and *B*: Cells were transfected with 15 MOI (ifu/cell) of β-gal, WT-p38α, and DN-p38α adenoviral constructs (*A*) or were treated without or with 10 μmol/L SB203580 for 30 min (*B*), before incubation without or with 5 nmol/L TNF for 30 min. Level of ErbB1-pTyr^{1173}, ErbB1-pTyr^{1086}, ErbB1, ErbB3-pTyr^{1289}, ErbB3, and MAPKAPK2-pThr^{334} were assessed using Western immunoblot analysis. *C*: Cells were treated without or with 25 μmol/L PD98059 (PD), 10 μmol/L SB203580, or 100 nmol/L wortmannin (Wort) for 30 min before incubation without or with 5 nmol/L TNF for 30 min. Akt activation was analyzed by immunoblotting with anti-Akt-pSer^{473} antibodies. Each panel in *A–C* contains a representative blot of three independent experiments. The RBI of a given band presents the means of three independent experiments, and intensity measurements were performed using ImageJ analysis. Mice model experiments: *D*: ErbB1-pTyr^{1173} and ErbB1 in the liver of C57 mice infected with β-gal (n = 10) or WT-p38α (n = 9) adenoviral constructs via tail vein injection were assessed using Western blot analysis. Quantification of immunoblots was performed using ImageJ analysis. The results are expressed as ErbB1-pTyr^{1173} relative to ErbB1 and are presented as the means ± SE. *E*: Levels of ErbB1-pTyr^{1173}, ErbB1, ErbB3-pTyr^{1289}, ErbB3, and α-tubulin in the liver of C57 mice fed with either standard diet (n = 5) or HFD (n = 5) were assessed using Western blot analysis. Quantification of immunoblots was performed using ImageJ analysis. The results are expressed as ErbB1-pTyr^{1173}, ErbB1, ErbB3-pTyr^{1289}, or ErbB3 relative to the loading control (α-tubulin) and are presented as the means ± SE.

under stress conditions, the ability of p38MAPK to promote IRS-1 Ser phosphorylation was evaluated in cells lacking ErbB receptors expression/activity. As depicted in Fig. 6*A*, knocking down ErbB1 by siRNA in HepG2 cells suppressed TNF effect on IRS-1 Ser phosphorylation without affecting TNF-induced p38MAPK phosphorylation. Similarly, simultaneous downregulation of ErbB2/ErbB3 expression in Fao cells (by culturing cells at low density [33]) attenuated AN-stimulated IRS-1 Ser phosphorylation, despite intact AN-induced p38MAPK activation (Fig. 6*B*). Similar findings were observed in HepG2 cells treated with PD168393, an ErbB1 Tyr kinase inhibitor, or in Fao cells treated with the ErbB2 kinase inhibitor AG825 (Supplementary Fig. 5).

Involvement of ROS in stress-induced ErbB receptors activation leading to insulin resistance. ROS had been suggested to mediate TNF-induced IRS-1 Ser phosphorylation in human hepatoma cells (34). Because exposure to

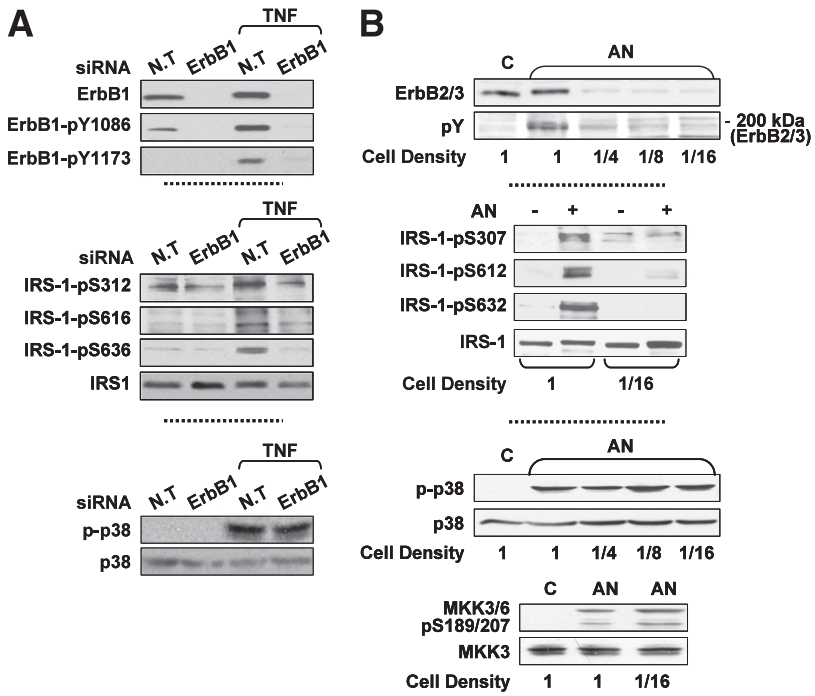

FIG. 6. The interrelationship between stress-induced ErbB Tyr phosphorylation, p38MAPK activation, and IRS-1 Ser phosphorylation. *A*: HepG2 cells transfected by nontargeted (N.T) or ErbB1 siRNA for 96 h were treated without or with 5 nmol/L TNF for 30 min at 37°C. ErbB1, ErbB1-pTyr^{1086}, ErbB1-pTyr^{1173}, IRS-1-pSer^{312}, IRS-1-pSer^{616}, IRS-1-pSer^{636}, IRS-1, *p*-p38, and p38 in total cell extract proteins were assessed using Western blot analysis. *B*: Fao cells, grown at various cell densities for 48 h, were incubated without or with 50 ng/mL AN for 30 min at 37°C. Particulate fractions were analyzed by immunoblot analysis using a mixture of anti-ErbB2 and anti-ErbB3 antibodies or anti-pTyr antibody. Cytosolic fractions were analyzed by immunoblot analysis using antibodies against IRS-1-pSer^{307}, IRS-1-pSer^{612}, IRS-1-pSer^{632}, IRS-1, *p*-p38, p38, MKK3/6 pSer$^{189/207}$, and MKK3. Each panel contains a representative blot of three to five independent experiments.

ROS had been demonstrated to enhance p38MAPK activation as well as ErbB receptors transactivation in various cellular models, we aimed at assessing whether the stress-induced p38MAPK-ErbB pathway leading to IRS-1 Ser phosphorylation is mediated by ROS. Indeed, TNF and AN promoted intracellular ROS generation in Fao cells, as demonstrated by increased oxidation of the redox-sensitive dye CM-DCF (Fig. 7*A*). Moreover, similar to our observations with TNF and AN, exposure of Fao cells to oxidative stress (treatment with GO in the presence of glucose) induced p38MAPK activation, ErbB2/ErbB3 transactivation, and IRS-1 Ser phosphorylation (Fig. 7*B*). ErbB2/ErbB3 transactivation by oxidative stress was supported by enhanced ErbB2/ErbB3 Tyr phosphorylation, coupled to increased association with PI3K and Akt activation (Fig. 7*C*). ErbB2/ErbB3 Tyr phosphorylation and IRS-1 Ser phosphorylation under oxidative stress followed in time course the activation of p38MAPK (Fig. 7*B*) and were almost completely abolished by p38MAPK inhibition (Fig. 7*D*). To further study the relevance of stress-induced ROS generation in p38MAPK-mediated ErbB2/ErbB3 transactivation, Fao cells were pretreated with different antioxidants before stress exposure. NAC and GSH, modulators of cellular thiol levels, and DPI, a general inhibitor of flavoprotein-containing oxidases (such as NADPH oxidase and nitric oxide synthase), significantly decreased the ability of AN (Fig. 7*E*), SMase, and TNF (data not shown) to induce ErbB2/ErbB3 transactivation, associated with significant inhibition in the activation of both p38MAPK and its upstream regulators MKK3/MKK6 (Fig. 7*E*). Additionally, NAC significantly decreased stress-induced IRS-1 Ser phosphorylation (Fig. 7*F*, *upper panels*) resulting in complete restoration of the in vitro interaction of IRS-1 with the IR (Fig. 7*F*, *lower panel*). Unlike stress-induced ErbB2/ErbB3 transactivation, ErbB2/ErbB3 Tyr phosphorylation, stimulated by the natural ligand NDF-β1, was unaffected by NAC, indicating that NAC does not inhibit ErbB2 tyrosine kinase activity per se (Fig. 7*G*). Collectively, these findings suggest a putative role for stress-induced ROS production in activation of the p38MAPK-ErbB cascade leading to insulin resistance.

DISCUSSION

The current study proposes new insight for the pivotal role of p38MAPK in the induction of insulin resistance; here we provide evidence that p38MAPK activation is required for ErbB receptors transactivation by various stresses, which then signals through a PI3K signaling cascade to promote insulin-signaling impairment (see suggested model in Fig. 8).

Several lines of evidence support this mechanism. First, stress stimuli including TNF, SMase, AN, and oxidative stress promoted p38MAPK activation in several hepatic cell lines, which paralleled in time course the ErbB receptors Tyr phosphorylation (ErbB 2/3 in Fao and ErbB1/3 in HepG2 cells). Second, inhibition of p38MAPK activity either by a pharmacological inhibitor, by DN-p38MAPKα, or by its silencing with specific p38MAPKα siRNA prevented the stress-induced ErbB receptors Tyr phosphorylation and their downstream signaling pathways. Correspondingly, inhibition of p38MAPK activation attenuated the stress-induced IRS-1 Ser phosphorylation on specific residues, which are known to mediate the stress-induced downregulation of insulin action (35–38). Indeed, p38MAPK inhibition improved IRS-1 ability to interact with IR and partially recovered Tyr phosphorylation of

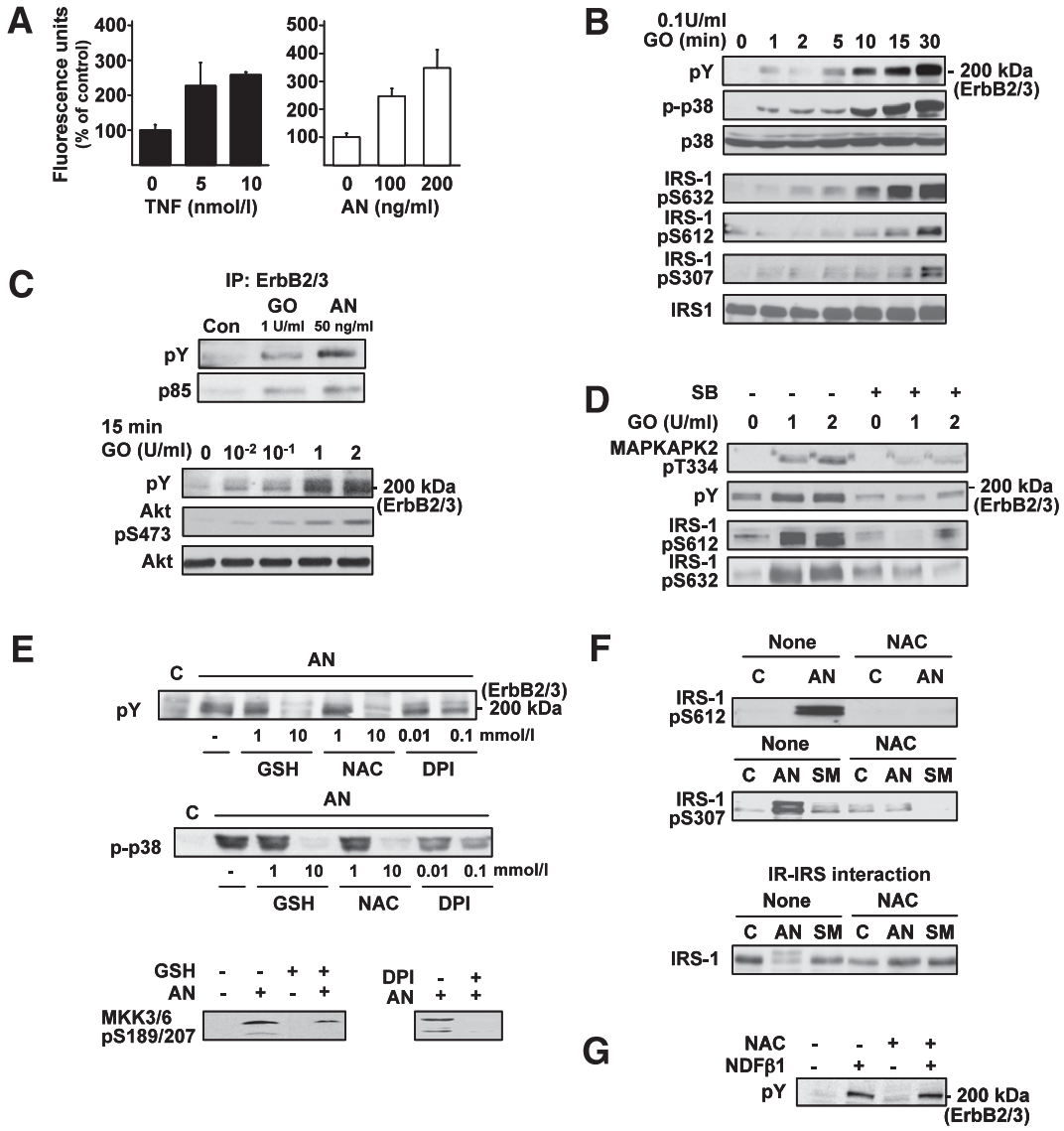

FIG. 7. Effects of ROS on stress-induced p38MAPK activation, ErbB2/ErbB3 transactivation, and IRS-1 Ser phosphorylation. *A*: ROS production in TNF- and AN-treated Fao cells was measured by the ROS-sensitive fluorescent dye CM-DCF. *B*: Particulate fraction proteins from Fao cells treated with 0.1 units/mL GO for the indicated times were analyzed by immunoblotting using anti-pTyr antibodies (*upper panel*), and the cytosolic fraction proteins were resolved by SDS-PAGE and then immunoblotted with antibodies as indicated. *C*: Fao cells were incubated with GO for the indicated doses for 15 min and with 50 ng/mL AN for 30 min. Proteins from cell lysates were immunoprecipitated by using a mixture of anti-ErbB2 and ErbB3 antibodies, resolved by SDS-PAGE, and immunoblotted with anti-pTyr or anti-p85 antibodies (*C*, *upper panels*) or directly resolved by SDS-PAGE and then immunoblotted with anti-pTyr, anti-Akt-pSer^{473}, and anti-Akt antibodies (*C*, *lower panels*). *D*: Total extracts, obtained from cells treated with 10 μmol/L SB203580 (SB) for 30 min before incubation with GO at the indicated doses, were resolved by SDS-PAGE and then immunoblotted with antibodies as indicated. *E*: Total proteins obtained from cells treated for 1 h without or with GSH, NAC, and DPI at the indicated doses (*upper panels*), or with 10 mmol/L GSH and 0.1 mmol/L DPI (*lower panel*) before incubation without or with 50 ng/mL AN for 30 min, were analyzed by immunoblot analysis using antibodies against pTyr, *p*-p38, and MKK3/6-pSer$^{189/207}$. *F*: Total proteins obtained from cells treated without or with 10 mmol/L NAC before incubation with 50 ng/mL AN or 300 mU/mL SMase as described above were analyzed by immunoblotting using anti-IRS-1-pSer^{612} and anti-IRS-1-pSer^{307} antibodies (*F*, *upper panels*). Cytosolic proteins obtained from cells treated without or with 10 mmol/L NAC for 1 h, and without or with AN or SMase, as described above, were bound to immobilized IR. IR-IRS complexes were resolved by SDS-PAGE and immunoblotted with anti-IRS-1 antibodies (*F*, *lower panel*). Each panel in *A–F* contains a representative blot of at least three independent experiments. *G*: Total proteins obtained from cells treated for 1 h without or with 10 mmol/L NAC before incubation with 50 ng/mL NDF-β1 for 15 min were analyzed by immunoblot analysis using antibodies against pTyr.

IRS-1 following insulin stimulation. The in vivo relevance of the suggested model is demonstrated by the beneficial effects of p38MAPKα attenuation on the improvement of metabolic derangements observed in an animal model for insulin resistance.

In support of the suggested mechanism, p38MAPK phosphorylation was found to be increased in the liver of *ob/ob* mice (26,27) and in skeletal muscle and adipocytes of type 2 diabetic patients (39,40), as well as in adipose tissue of Zucker obese rats, where treatment with rosiglitazone decreased its activation accompanied by reduced IRS-1 Ser phosphorylation (41). Furthermore, p38MAPK-dependent phosphorylation of Ser^{307} was reported in rat myotubes chronically exposed to TNF (19) and inhibition of p38MAPK under oxidative conditions or treatment with the antioxidant α-lipoic acid restored insulin sensitivity (14,42).

The precise function of p38MAPK or its downstream effectors in mediating ligand-independent ErbB receptors

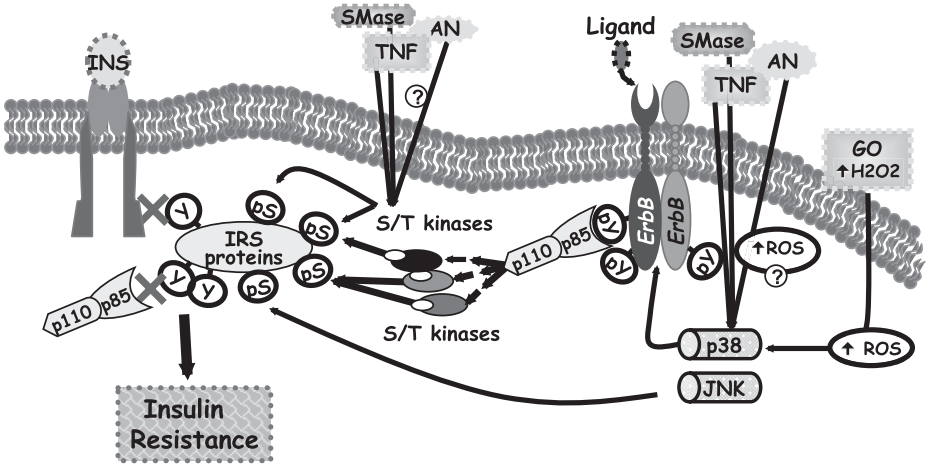

FIG. 8. A model illustrating the role of p38MAPK in liver stress-induced insulin resistance. Stress-induced p38MAPK activation is upstream to ErbB receptors transactivation and leads to IRS-1 Ser phosphorylation and insulin signaling desensitization. Stress-induced IRS-1 Ser phosphorylation can be mediated by additional pathways that activate various IRS-1 kinases and may possibly be associated with intracellular ROS generation.

activation in the liver is currently unclear. A possible mechanism may be suggested by the observation that in cells exposed to oxidative stress specific Tyr phosphatases were neutralized by p38MAPK, leading to sustained Tyr phosphorylation of ErbB1 (43). Other reports have demonstrated that stress stimuli, including SMase, H_2O_2, and heat shock, mediate the activation of ErbB proteins through nonreceptor Tyr kinases such as Src and Pyk2 (44–46), although the role of p38MAPK in activation of these kinases is not established. A third potential mechanism was suggested by the observation that, under stress conditions, p38MAPK mediates metalloprotease activation and proteolytic processing of pro-HB-EGF ligand precursors, leading to ErbB1 transactivation (23). Recent studies demonstrated that stress-induced p38MAPK pathway mediates ErbB1 phosphorylation on several Ser/Thr residues located at the carboxy-terminal tail of the receptor (47); however, the relevance of such an event to ErbB receptors transactivation is not clear. Further studies will be necessary to identify the pathways that link p38MAPK to ErbB receptors transactivation.

Increased ROS levels by TNF had been shown to be an important trigger for insulin resistance (5). Our findings of increased ROS production by stress stimuli, p38MAPK-ErbB pathway activation by oxidative stress and the ability of antioxidants to restore insulin sensitivity following exposure to stress stimuli, point to a potential role of ROS generation in mediating stress-induced p38MAPK-ErbB receptors activation leading to insulin resistance (Fig. 8). Such a mechanism is supported by the observation that TNF induces insulin resistance in hepatic cells through increased ROS production, which results in sustained activation of ASK1 (34), an upstream activator of the MKK3/MKK6-p38MAPK cascade (48), and the finding that EGF-receptor transactivation by TNF is regulated in a redox-dependent manner (49). In addition, ROS production in response to TNF had been shown to inactivate MAPK phosphatases leading to sustained MAPK activation (50). The possibility that ROS generation, in response to stress stimuli, may promote IRS-1 Ser phosphorylation through stimulation of additional signaling pathways cannot be excluded, since the antioxidant NAC attenuated not only p38MAPK activation but also JNK activation (results not shown). Whereas JNK promotes TNF- and AN-induced insulin resistance by direct association with IRS-1 and phosphorylation of Ser^{307} (15,51), our findings demonstrate that p38MAPK regulates IRS-1 Ser phosphorylation indirectly through ErbB receptors activation of downstream kinases. Thus stress-induced IRS-1 Ser phosphorylation may be triggered by multiple pathways activating different IRS-1 kinases (38), which act in concert to impair insulin action (Fig. 8). Further studies will be required to establish the potential linkage between ROS generation and the p38MAPK-ErbB cascade in insulin resistance induction.

In conclusion, the current study suggests a novel mechanism underlying the development of hepatic insulin resistance under cellular stress conditions. In response to different stress stimuli, p38MAPK activation initiates ErbB receptors signaling, leading to Ser phosphorylation of IRS proteins and impaired cellular response to insulin. This may provide a mechanism which enables diversion of cell machinery from controlled nutrient transport and anabolism to that of survival, growth, and repair. Further studies will be required to assess the relevance of the proposed mechanism in other insulin target tissues.

ACKNOWLEDGMENTS

This work was supported in part by Research Grant 3/4039 from the Chief Scientist's Office of the Ministry of Health, Israel (to H.K. and R.H.) and from the D-Cure Foundation for Diabetes Care in Israel (to H.K. and R.H.). This work was performed in partial fulfillment of the requirements for the PhD degree for Y.Y. and E.B. (The Mina and Everard Goodman Faculty of Life Sciences, Bar-Ilan University, Ramat-Gan, Israel).

No potential conflicts of interest relevant to this article were reported.

R.H., Y.Y., and E.B. researched data, contributed to discussion, wrote the manuscript, and reviewed and edited the manuscript. M.K.-M. researched data, contributed to discussion, and wrote the manuscript. A.K. contributed to discussion. A.T. and H.K. contributed to discussion, wrote the manuscript, and reviewed and edited the manuscript.

The authors thank Prof. Jiahuai Han (The Scripps Research Institute, La Jolla, CA) for providing the adenoviral

constructs for DN- and WT-p38MAPKα. The authors appreciate the helpful advice and assistance of Prof. Zecharia Madar (Hebrew University of Jerusalem, Israel) and Dr. Aviv Shaish (Institute of Lipid and Atherosclerosis Research, Sheba Medical Center, Israel) in the animal studies.

REFERENCES

1. Kahn BB, Flier JS. Obesity and insulin resistance. J Clin Invest 2000;106:473–481
2. Del Aguila LF, Krishnan RK, Ulbrecht JS, et al. Muscle damage impairs insulin stimulation of IRS-1, PI 3-kinase, and Akt-kinase in human skeletal muscle. Am J Physiol Endocrinol Metab 2000;279:E206–E212
3. Ikezu T, Okamoto T, Yonezawa K, Tompkins RG, Martyn JA. Analysis of thermal injury-induced insulin resistance in rodents. Implication of post-receptor mechanisms. J Biol Chem 1997;272:25289–25295
4. Ma Y, Toth B, Keeton AB, Holland LT, Chaudry IH, Messina JL. Mechanisms of hemorrhage-induced hepatic insulin resistance: role of tumor necrosis factor-alpha. Endocrinology 2004;145:5168–5176
5. Houstis N, Rosen ED, Lander ES. Reactive oxygen species have a causal role in multiple forms of insulin resistance. Nature 2006;440:944–948
6. Esposito KNF, Nappo F, Marfella R, et al. Inflammatory cytokine concentrations are acutely increased by hyperglycemia in humans: role of oxidative stress. Circulation 2002;106:2067–2072
7. Wellen KE, Hotamisligil GS. Inflammation, stress, and diabetes. J Clin Invest 2005;115:1111–1119
8. Shoelson SE, Lee J, Goldfine AB. Inflammation and insulin resistance. J Clin Invest 2006;116:1793–1801
9. Kanety H, Feinstein R, Papa MZ, Hemi R, Karasik A. Tumor necrosis factor alpha-induced phosphorylation of insulin receptor substrate-1 (IRS-1). Possible mechanism for suppression of insulin-stimulated tyrosine phosphorylation of IRS-1. J Biol Chem 1995;270:23780–23784
10. Hotamisligil GS, Peraldi P, Budavari A, Ellis R, White MF, Spiegelman BM. IRS-1-mediated inhibition of insulin receptor tyrosine kinase activity in TNF-alpha- and obesity-induced insulin resistance. Science 1996;271:665–668
11. Paz K, Hemi R, LeRoith D, et al. A molecular basis for insulin resistance. Elevated serine/threonine phosphorylation of IRS-1 and IRS-2 inhibits their binding to the juxtamembrane region of the insulin receptor and impairs their ability to undergo insulin-induced tyrosine phosphorylation. J Biol Chem 1997;272:29911–29918
12. Kanety H, Hemi R, Papa MZ, Karasik A. Sphingomyelinase and ceramide suppress insulin-induced tyrosine phosphorylation of the insulin receptor substrate-1. J Biol Chem 1996;271:9895–9897
13. Rudich A, Tirosh A, Potashnik R, Hemi R, Kanety H, Bashan N. Prolonged oxidative stress impairs insulin-induced GLUT4 translocation in 3T3-L1 adipocytes. Diabetes 1998;47:1562–1569
14. Maddux BA, See W, Lawrence JC Jr, Goldfine AL, Goldfine ID, Evans JL. Protection against oxidative stress-induced insulin resistance in rat L6 muscle cells by mircomolar concentrations of α-lipoic acid. Diabetes 2001;50:404–410
15. Aguirre V, Uchida T, Yenush L, Davis R, White MF. The c-Jun NH(2)-terminal kinase promotes insulin resistance during association with insulin receptor substrate-1 and phosphorylation of Ser(307). J Biol Chem 2000;275:9047–9054
16. Hemi R, Paz K, Wertheim N, Karasik A, Zick Y, Kanety H. Transactivation of ErbB2 and ErbB3 by tumor necrosis factor-alpha and anisomycin leads to impaired insulin signaling through serine/threonine phosphorylation of IRS proteins. J Biol Chem 2002;277:8961–8969
17. Gual P, Gonzalez T, Gremeaux T, Barres R, Le Marchand-Brustel Y, Tanti JF. Hyperosmotic stress inhibits insulin receptor substrate-1 function by distinct mechanisms in 3T3-L1 adipocytes. J Biol Chem 2003;278:26550–26557
18. Fujishiro M, Gotoh Y, Katagiri H, et al. Three mitogen-activated protein kinases inhibit insulin signaling by different mechanisms in 3T3-L1 adipocytes. Mol Endocrinol 2003;17:487–497
19. de Alvaro C, Teruel T, Hernandez R, Lorenzo M. Tumor necrosis factor alpha produces insulin resistance in skeletal muscle by activation of inhibitor kappaB kinase in a p38 MAPK-dependent manner. J Biol Chem 2004;279:17070–17078
20. Li G, Barrett EJ, Barrett MO, Cao W, Liu Z. Tumor necrosis factor-alpha induces insulin resistance in endothelial cells via a p38 mitogen-activated protein kinase-dependent pathway. Endocrinology 2007;148:3356–3363
21. Ono K, Han J. The p38 signal transduction pathway: activation and function. Cell Signal 2000;12:1–13
22. Cheng H, Kartenbeck J, Kabsch K, Mao X, Marqués M, Alonso A. Stress kinase p38 mediates EGFR transactivation by hyperosmolar concentrations of sorbitol. J Cell Physiol 2002;192:234–243
23. Fischer OM, Hart S, Gschwind A, Prenzel N, Ullrich A. Oxidative and osmotic stress signaling in tumor cells is mediated by ADAM proteases and heparin-binding epidermal growth factor. Mol Cell Biol 2004;24:5172–5183
24. Huang S, Jiang Y, Li Z, et al. Apoptosis signaling pathway in T cells is composed of ICE/Ced-3 family proteases and MAP kinase kinase 6b. Immunity 1997;6:739–749
25. Jiang S, Gavrikova TA, Pereboev A, Messina JL. Adenovirus infection results in alterations of insulin signaling and glucose homeostasis. Am J Physiol Endocrinol Metab 2010;298:E1295–E1304
26. Gum RJ, Gaede LL, Heindel MA, et al. Antisense protein tyrosine phosphatase 1B reverses activation of p38 mitogen-activated protein kinase in liver of ob/ob mice. Mol Endocrinol 2003;17:1131–1143
27. Kondo T, Kahn CR. Altered insulin signaling in retinal tissue in diabetic states. J Biol Chem 2004;279:37997–38006
28. Nakatani Y, Kaneto H, Kawamori D, et al. Modulation of the JNK pathway in liver affects insulin resistance status. J Biol Chem 2004;279:45803–45809
29. Keeton AB, Amsler MO, Venable DY, Messina JL. Insulin signal transduction pathways and insulin-induced gene expression. J Biol Chem 2002;277:48565–48573
30. Keeton AB, Bortoff KD, Bennett WL, Franklin JL, Venable DY, Messina JL. Insulin-regulated expression of Egr-1 and Krox20: dependence on ERK1/2 and interaction with p38 and PI3-kinase pathways. Endocrinology 2003;144:5402–5410
31. Qiao L, MacDougald OA, Shao J. CCAAT/enhancer-binding protein alpha mediates induction of hepatic phosphoenolpyruvate carboxykinase by p38 mitogen-activated protein kinase. J Biol Chem 2006;281:24390–24397
32. Liu HY, Collins QF, Xiong Y, et al. Prolonged treatment of primary hepatocytes with oleate induces insulin resistance through p38 mitogen-activated protein kinase. J Biol Chem 2007;282:14205–14212
33. Kornilova ES, Taverna D, Hoeck W, Hynes NE. Surface expression of erbB-2 protein is post-transcriptionally regulated in mammary epithelial cells by epidermal growth factor and by the culture density. Oncogene 1992;7:511–519
34. Imoto K, Kukidome D, Nishikawa T, et al. Impact of mitochondrial reactive oxygen species and apoptosis signal-regulating kinase 1 on insulin signaling. Diabetes 2006;55:1197–1204
35. De Fea K, Roth RA. Modulation of insulin receptor substrate-1 tyrosine phosphorylation and function by mitogen-activated protein kinase. J Biol Chem 1997;272:31400–31406
36. Aguirre V, Werner ED, Giraud J, Lee YH, Shoelson SE, White MF. Phosphorylation of Ser307 in insulin receptor substrate-1 blocks interactions with the insulin receptor and inhibits insulin action. J Biol Chem 2002;277:1531–1537
37. Weigert C, Kron M, Kalbacher H, et al. Interplay and effects of temporal changes in the phosphorylation state of serine-302, -307, and -318 of insulin receptor substrate-1 on insulin action in skeletal muscle cells. Mol Endocrinol 2008;22:2729–2740
38. Boura-Halfon S, Zick Y. Phosphorylation of IRS proteins, insulin action, and insulin resistance. Am J Physiol Endocrinol Metab 2009;296:E581–E591
39. Koistinen HA, Chibalin AV, Zierath JR. Aberrant p38 mitogen-activated protein kinase signalling in skeletal muscle from Type 2 diabetic patients. Diabetologia 2003;46:1324–1328
40. Carlson CJ, Koterski S, Sciotti RJ, Poccard GB, Rondinone CM. Enhanced basal activation of mitogen-activated protein kinases in adipocytes from type 2 diabetes: potential role of p38 in the downregulation of GLUT4 expression. Diabetes 2003;52:634–641
41. Jiang G, Dallas-Yang Q, Biswas S, Li Z, Zhang BB. Rosiglitazone, an agonist of peroxisome-proliferator-activated receptor gamma (PPARgamma), decreases inhibitory serine phosphorylation of IRS1 in vitro and in vivo. Biochem J 2004;377:339–346
42. Blair AS, Hajduch E, Litherland GJ, Hundal HS. Regulation of glucose transport and glycogen synthesis in L6 muscle cells during oxidative stress. Evidence for cross-talk between the insulin and SAPK2/p38 mitogen-activated protein kinase signaling pathways. J Biol Chem 1999;274:36293–36299
43. Ruano MJ, Hernández-Hernando S, Jiménez A, Estrada C, Villalobo A. Nitric oxide-induced epidermal growth factor-dependent phosphorylations in A431 tumour cells. Eur J Biochem 2003;270:1828–1837
44. Emkey R, Kahn CR. Cross-talk between phorbol ester-mediated signaling and tyrosine kinase proto-oncogenes. II. Comparison of phorbol ester and

sphingomyelinase-induced phosphorylation of ErbB2 and ErbB3. J Biol Chem 1997;272:31182–31189
45. Wang XT, McCullough KD, Wang XJ, Carpenter G, Holbrook NJ. Oxidative stress-induced phospholipase C-gamma 1 activation enhances cell survival. J Biol Chem 2001;276:28364–28371
46. Lin RZ, Hu ZW, Chin JH, Hoffman BB. Heat shock activates c-Src tyrosine kinases and phosphatidylinositol 3-kinase in NIH3T3 fibroblasts. J Biol Chem 1997;272:31196–31202
47. Zwang Y, Yarden Y. p38 MAP kinase mediates stress-induced internalization of EGFR: implications for cancer chemotherapy. EMBO J 2006;25:4195–4206
48. Rudich A, Kanety H, Bashan N. Adipose stress-sensing kinases: linking obesity to malfunction. Trends Endocrinol Metab 2007;18:291–299
49. Hirota K, Murata M, Itoh T, Yodoi J, Fukuda K. Redox-sensitive transactivation of epidermal growth factor receptor by tumor necrosis factor confers the NF-kappa B activation. J Biol Chem 2001;276:25953–25958
50. Kamata H, Honda S, Maeda S, Chang L, Hirata H, Karin M. Reactive oxygen species promote TNFalpha-induced death and sustained JNK activation by inhibiting MAP kinase phosphatases. Cell 2005;120:649–661
51. Hirosumi J, Tuncman G, Chang L, et al. A central role for JNK in obesity and insulin resistance. Nature 2002;420:333–336